Mixed-Oxide Pillared Silicates from H-Ilerite by Intercalation

Katsunori Kosuge* and Puyam S. Singh†

Materials Processing Department, National Institute for Resources and Environment, 16-3 Onogawa, Tsukuba-shi, Ibaraki, 305-8569 Japan

Received July 19, 1999

Al-, Ti-, and Zr-containing silica-based pillars of which Si^{4+} is isomorphously substituted by each ion have been formed between the silicate layers of H-ilerite by intercalation of octylamine and mixed alkoxides. The resultant silica-based pillared materials have a BET surface area of about 800 m^2/g at 600 °C and have the gallery heights of 2−3 nm and micropores of >2 nm in size between the silicate layers. The increase in the amount of metal introduced into the silica-based pillars was accompanied by a change in the pillar configuration, which led to the formation of the microporous products with uniform pore diameters of ∼0.90 nm and the irregular gallery height. The ^{29}Si MAS NMR, ^{27}Al MAS NMR, and UV−vis spectra revealed the incorporation of Al, Ti, and Zr atoms as isolated elemental sites into the silicate pillar framework.

Introduction

Among the available layered compounds, smectite clay minerals that easily swell in water have received the most attention and seem to have great potential in the area of pillared materials.[1] However, the pillaring procedures based on the direct ion exchange of interlayer cations with hydrated polycations developed for clay minerals have not been generally applicable to the wide variety of layered metal oxides due to the high charge density on the framework. Some researchers reported the synthesis of pillared compounds from layered metal oxides by utilizing a preswelling step in which the interlayer is intercalated with organoammonium ions.[2] Alkylamines readily intercalate and increase the interlayer distance depending on the alkyl chain length. The opened layers then facilitate the replacement of alkylammonium ions by the large inorganic cations or the precursors of the pillars. Landis et al.[3] have used the interlayer hydrolysis of tetraethyl orthosilicate (TEOS) on the primary organoammonium-exchanged forms to prepare silica-pillared materials of a wide variety of layered metal oxides, including the layered silicic acids[4] of magadiite ($Na_2Si_{14}O_{29}\cdot H_2O$) and kenyaite ($Na_2Si_{22}O_{45}\cdot H_2O$). Layered silicic acids, which are easily derived from layered silicates such as magadiite, kenyaite, and ilerite ($Na_2Si_8O_{17}\cdot H_2O$)[5,6] by proton exchange, are found to be very useful hosts in the formation of pillared materials due to the presence of reactive silanol groups on their interlayer surface.[4,5,7] Silanol groups, which are acidic enough to allow proton transfer to an amine group,[8] are oriented in a crystallographically regular manner on the interlayer surface.[6,7] Consequently, such groups will easily provide a porous material with a high degree of uniformity during the pillar formation.[9,10] In addition, pillared products induced by silicic acids are highly heat resistant upon calcination since the silicate framework contains neither OH groups nor other cations.[10] On the basis of the preswelling step procedure developed by Landis et al., various silica-pillared products have been synthesized from the layered silicic acids[9,10,11] and different types of layered materials.[3,12]

In the case of non-silica pillared silicic acids, only Al-pillared magadiite has been prepared by utilizing a preswelling step.[13] On the other hand, many kinds of oxides such as Al_2O_3, TiO_2, ZrO_2, etc., which have several significant and distinctive properties as a catalyst or catalyst support, have been formed as a pillar between the layers of smectite clay minerals by a direct

* To whom correspondence should be addressed. Telephone: 81-298-58-8492. Fax: 81-298-58-8459. E-mail: kosuge@nire.go.jp.

† Current address: Physical and Theoretical Chemistry Section, Research School of Chemistry, Australian National University, ACT 0200, Canberra.

(1) Occelli, M. L., Robson, H. E., Eds. *Expanded Clays and Other Microporous Solids*; Van Nostrand Reinhold: New York, 1992.

(2) (a) Clearfield, A.; Roberts, B. D. *Inorg. Chem.* **1988**, *27*, 3237. (b) Cheng, S.; Wang, T. C. *Inorg. Chem.* **1989**, *28*, 1283. (c) Anderson, M. W.; Klinowski, J. *Inorg. Chem.* **1990**, *29*, 3260.

(3) Landis, M. E.; Aufdembrink, B. A.; Chu, P.; Johnson, I. D.; Kirker, G. W.; Rubin, M. K. *J. Am. Chem. Soc.* **1991**, *113*, 3189.

(4) (a) Lagaly, G. *Adv. Colloid Interface Sci.* **1979**, *11*, 105. (b) Lagaly, G.; Beneke, K. *Colloid. Polym. Sci.* **1991**, *269*, 1198.

(5) Borbely, G.; Beyer, H. K.; Karge, H. G.; Schwieger, W.; Brandt, A.; Bergk, K.-H. *Clays Clay Miner.* **1991**, *39*, 490.

(6) Vortmann, S.; Rius, J.; Siegmann, S.; Gies, H. *J. Phys. Chem. B* **1997**, *101*, 1292.

(7) Rojo, J. M.; Ruiz-Hitzky, E.; Sanz, J.; Serratosa, J. M. *Rev. Chim. Miner.* **1983**, *20*, 807.

(8) Lagaly, G. *Solid State Ionics* **1986**, *22*, 43.

(9) Dailey, J. S.; Pinnavaia, T. J. *Chem. Mater.* **1992**, *4*, 855.

(10) Kosuge, K.; Tsunashima, A. *J. Chem. Soc., Chem. Commun.* **1995**, 2427.

(11) (a) Kwon, O. Y.; Jeong, S. Y.; Suh, J. K.; Ryu, B. H.; Lee, J. M. *J. Colloid Interface Sci.* **1996**, *177*, 677. (b) Jeong, S. Y.; Suh, J. K.; Jin, H.; Lee, J. M.; Kwon, O. Y. *J. Colloid Interface Sci.* **1996**, *180*, 269.

(12) (a) Domen, K.; Ebina, Y.; Sekine, T.; Tanaka, A.; Kondo, J.; Hirose, C. *Catal. Today* **1993**, *16*, 479. (b) Shangguan, W.; Inoue, K.; Yoshida, A. *J. Chem. Soc., Chem. Commun.* **1998**, 779. (c) Yamanaka, S.; Kunii, K.; Xu, Z. L. *Chem. Mater.* **1998**, *10*, 1931.

(13) Wong, S. H.; Cheng, S. *Chem. Mater.* **1993**, *5*, 770.

10.1021/cm990451m CCC: $19.00
Published on Web 01/27/2000

ion-exchange procedure with hydrated polycations.[1,12] Furthermore, it is well-known that transition metals, which are isomorphously substituted for Si^{4+} in the silicate framework, play a significant role in catalytic oxidation reactions such as the liquid-phase epoxidation of various organic substrates and photocatalytic degradation of environmental pollutants.[14,15] However, there have been few studies about the synthesis of the silica-based oxide pillared compounds even for smectite.

In the present study we report the synthesis of Ti-, Zr-, and Al-containing silica-pillared materials using the silicic acid of ilerite as a host at ambient temperature by a modified procedure developed by Landis et al. The physicochemical properties of the products are characterized by XRD, nitrogen adsorption, ^{29}Si and ^{27}Al solid-state MAS NMR, and UV−vis spectroscopy. Furthermore, the catalytic activities are evaluated for the peroxide epoxidation of olefins for the Ti−Si mixed-pillared products.

Experimental Section

Materials Synthesis. The silicic acid of ilerite (designated H-ilerite) used in this study as a host material was prepared as described in our previous study.[10] The Ti−Si mixed-oxide pillared product was synthesized by the following method. A 0.25 g sample of H-ilerite was dispersed in octylamine (2 mL) at room temperature for 24 h. After 1 day, the mixed solution with a definite molar ratio of tetraethyl orthosilicate (TEOS), tetraethylorthotitanate (TEOT), and octylamine was stirred for 20 min. The mixed alkoxide solution was then added to the composite of the octylamine-intercalated H-ilerite and reacted at room temperature for 6 h with stirring. The resultant product was centrifuged and air-dried at room temperature for 48 h. The final white product was obtained by calcination in air at 600 °C for 1 h. The Zr−Si and Al−Si mixed-oxide pillared products were synthesized in a similar manner using zirconium butoxide containing 80 wt % solution in 1-butanol and aluminum tri-*sec*-butoxide as the alkoxide sources, respectively. For comparison, the pure silica-pillared material was also prepared in the same manner only using TEOS. The molar ratio of Si to octylamine in every suspension is ca. 1:0.7, and the molar % of metal with respect to Si is given in Table 1. In the following sections, the mixed-oxide pillared product is designated as M−SiHIP(x) where M represents Ti, Zr, and Al, and x means the mol % of the metal in total silicon content of the starting mixture of alkoxides. The pure silica-pillared product is described as Si−HIP. These designated descriptions will be used for both the intercalated compounds before and after calcination.

Characterization. The powder X-ray diffraction (XRD) patterns were obtained with a Rigaku Rotaflex diffractometer equipped with a rotating anode and Cu Kα radiation (wavelength = 0.1542 nm).

Transmission electron microscopy (TEM) images were obtained using a JEOL 2000FX. Solid-state MAS NMR spectra were recorded on a CMX 300 MHz NMR spectrometer using 7.5 mm zirconia rotors for ^{29}Si and 4 mm for ^{27}Al at 59.71 MHz. The sample spinning frequency for the ^{29}Si MAS NMR measurements was 3 kHz using 90° pulses at 600 s intervals with high-power proton decoupling. The ^{29}Si CP MAS NMR spectra were recorded using a 4 ms contact time, a 5 s recycling delay time, and 2000 scans. The ^{27}Al solid-state MAS NMR spectra were measured using 4.0 mm zirconia rotors spinning at 12 kHz using 90° pulses at 180 s intervals with high power proton decoupling. Prior to the ^{27}Al MAS NMR experiments, all calcined samples were kept for 48 h in air at room temperature.

UV−vis diffuse reflectance spectra were measured at room temperature on a Shimadzu UV-2500 equipped with an integrating sphere using $BaSO_4$ as a reference.

The N_2 isotherms were obtained at −196 °C on BELSORP 28 under continuous adsorption conditions. Prior to the measurements, samples were heated at 200 °C for 2 h, and finally outgassed at 10^{-3} Torr at room temperature. The BET and t plot analyses were used to calculate the total specific surface area (S_{BET}), micropore surface area (S_{int}), and micropore volume (V) of the products.[16] The mean pore diameter of the products were determined by the MP plot for micropores.[17]

Catalytic Experiments. After the Ti−SiHIP samples were pretreated in a static atmosphere at 600 °C for 1 h, 0.05 g of Ti−SiHIP was mixed with 25 mmol of olefins and 5 mmol of anhydrous *tert*-butyl hydroperoxide (TBHP) in decane (5−6 M, Aldrich). The oxidation reactions were carried out at 60 °C for 5 h with stirring in a one-necked round-bottom glass flask with a chilled condenser. The products were analyzed by gas chromatography equipped with a capillary column (5% methylpenylsilicone, 25m length) and a FID detector.

Table 1. Porous Properties of Mixed-Oxides Pillared Silicates from H-Ilerite by Intercalation

element	calcined T (°C)	mol %[a]	S_{BET} ($m^2\ g^{-1}$)	S_{int} ($m^2\ g^{-1}$)	V (mL g^{-1})	D (nm)
Si	600		956		0.58	
Si	800		728		0.43	
Ti	600	0.98	874	860	0.41	0.90
Ti	600	1.98	837	829	0.37	0.90
Ti	800	1.98	486	480	0.19	0.90
Al	600	0.79	876		0.54	
Al	600	2.00	806		0.53	
Al	800	2.00	715		0.42	
Al	600	4.48	624	604	0.29	0.90
Zr	600	0.94	902		0.54	
Zr	600	1.89	881		0.54	
Zr	800	1.89	664		0.38	
Zr	600	4.57	795	786	0.39	0.95

[a] Mol % = (metal/silicon) × 100.

Results and Discussion

X-ray Powder Diffraction and TEM. Figure 1A shows the XRD patterns of the basal reflections for the calcined products at 600 °C, and the representative XRD patterns of the as-synthesized composites and the corresponding calcined products at a higher 2θ region are presented in Figure 1B. Since the basal spacing (d_{001}) of the calcined composites are about 5 times larger than d_{001} = 0.74 nm of H-ilerite, the pillar structures are found to be formed between the silicate layers for every calcined product by the intercalation procedure. The expansion of the silicate layers by intercalation can be evidenced by direct examination of the lattice fringe image spacing using the high-resolution transmission electron micrograph (HRTEM) image as shown in Figure 2. The micrograph for Si−HIP reveals almost the same interlayer distance of ∼2.5 nm in almost the entire crystals as shown in Figure 2a. In contrast to Si−HIP,

(14) (a) Yang, R. T.; Cheng, L S. *Access in Nanoporous Materials. Pillared Clays and Ion-Exchanged Pillared Clays as Gas Adsorbents and as Catalysts for Selective Catalytic Reduction of NO*; Plenum Press: New York, 1995; pp 73−92. (b) Corma, A. *Chem. Rev.* **1997**, *97*, 2373.

(15) (a) Szostak, R. *Molecular Sieves. Principles of Synthesis and Identification*; Van Nostrand Reinhold: New York, 1989; pp 205−281. (b) Sayari, A. *Chem. Mater.* **1996**, *8*, 1840. (c) Tatsumi, T. *Curr. Opin. Solid State Mater. Sci.* **1997**, *2*, 76.

(16) Gregg, S. G.; Sing, K. S. W. *Adsorption Surface Area and Porosity*, 2nd ed.; Academic Press: New York, 1982.

(17) Mikhail, R. S. H.; Brunauer, S.; Bodor, E. E. *J. Colloid Interface Sci.* **1968**, *26*, 45.

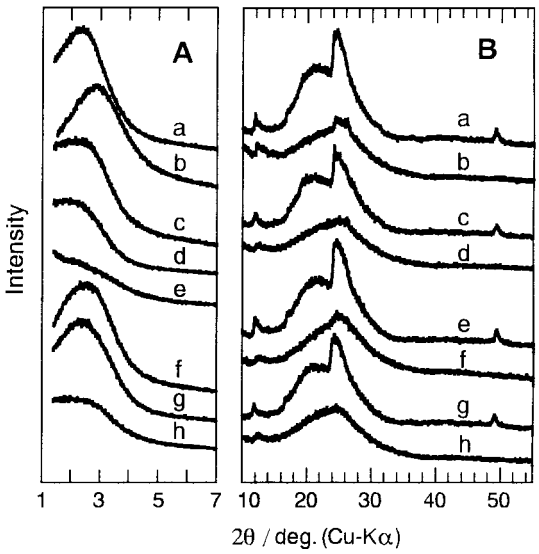

Figure 1. (A) Basal X-ray diffraction reflections of (a) Si−HIP, (b) Ti−SiHIP(1.98), (c) Al−SiHIP(0.79), (d) Al−SiHIP-(2.00), (e) Al−SiHIP(4.48), (f) Zr−SiHIP(0.94), (g) Zr−SiHIP-(1.89), and (h) Zr−SiHIP(4.57) calcined at 600 °C; and (B) wide-angle XRD patterns of the as-synthesized and calcined samples: (a) Si−HIP, (c) Ti−SiHIP(1.98), (e) Zr−SiHIP(1.89), and (g) Al−SiHIP(2.00) are as-synthesized samples, and b, d, f, and h are the corresponding calcined products at 600 °C.

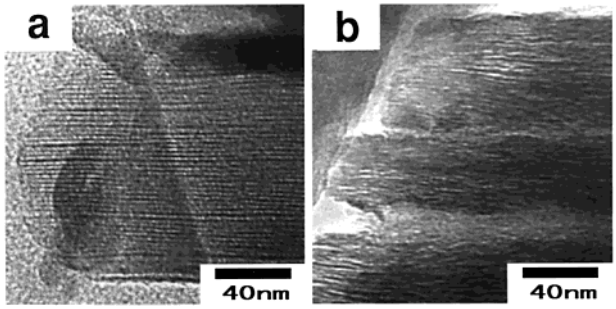

Figure 2. Transmission electron microscopy images of calcined products for (a) Si−HIP and (b) Ti−SiHIP(1.98).

less homogeneity was observed in the micrograph for every mixed oxides pillared product. The HRTEM image of Ti−SiHIP(1.98) is shown in Figure 2b. The reduced uniformity of the interlayer distance for the silica-based pillared products should be consistent with the significant broadness in the XRD patterns of the basal reflections than that of Si−HIP. In addition, by increasing the amount of each metal introduced into the pillar structure, the basal reflections tend to become much broader. On the basis of the unit silicate layer thickness of 0.72 nm in H-ilerite,[6] the range of mean gallery heights for the pillared product is 2−3 nm. Furthermore, the peaks at $2\theta = 24-26°$ for every calcined product became more obscure than that of Si−HIP upon calcination although little difference among the XRD patterns of the as-synthesized products was recognized (Figure 1B). The broad peak at $2\theta = 15-35°$ for every calcined product might be ascribed to the amorphous phase as a pillar formed between the interlayers.

These XRD patterns as mentioned above may indicate that the silica-based mixed-oxide pillared products have less ordered stacking layers in both directions of vertical and horizontal than those of Si−HIP, which is consistent with the reduced uniformity of the HRTEM image as shown in Figure 2b.

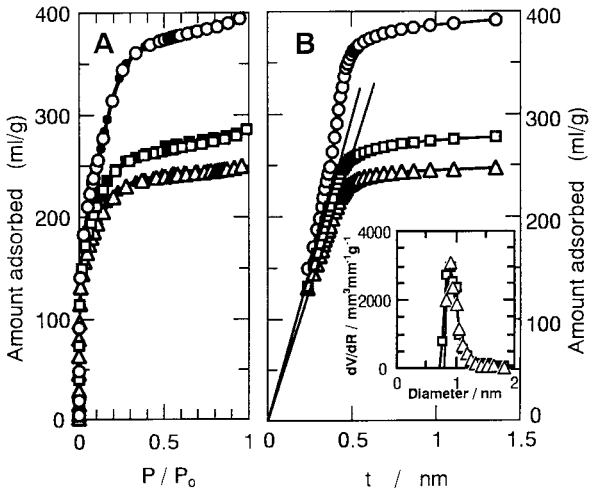

Figure 3. (A) Nitrogen adsorption and desorption isotherms of calcined products at 600 °C of (○) Si−HIP, (□) Ti−SiHIP-(0.98), and (△) Ti−SiHIP(1.98); and (B) the corresponding *t* curves and MP plots of A.

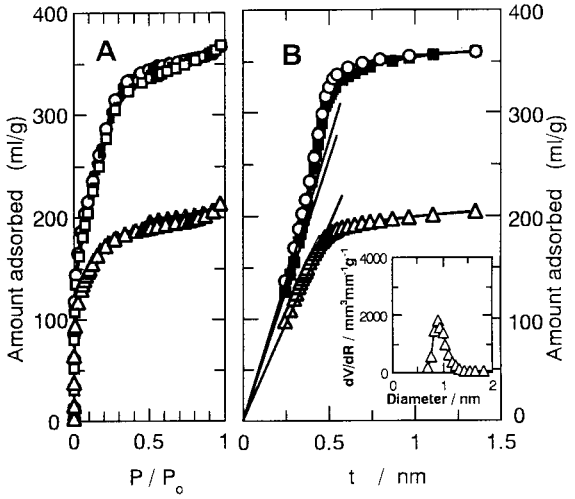

Figure 4. (A) Nitrogen adsorption and desorption isotherms of calcined Al−SiHIP(*x*) at 600 °C with $x =$ (○) 0.79, (□) 2.00, and (△) 4.48; and (B) the corresponding *t* curves and MP plots of A.

N_2 Isotherms. Figures 3A, 4A, and 5A show the N_2 adsorption−desorption isotherms of the calcined products at 600 °C. The corresponding *t* curves[16] are shown in Figures 3B, 4B, and 5B. From the isotherms, little hysteresis loops and no steps at high relative pressure are observed for each product, indicating that silica and the silica-based mixed-oxide pillared materials have few external surfaces between the particles. The isotherm of Si−HIP is classified into type I on the basis of the BDDT classification as shown in Figure 3A.[16,18] However, the corresponding *t* curve has an upward swing from linearity below the downward bend due to saturated filling (Figure 3B). This phenomenon would be attributed to the micropores whose pore width is < 2 nm.[19] Al−SiHIP(0.79, and 2.00) and Zr−SiHIP(0.94, and 1.89) with a lower content of Al and Zr exhibit a similar behavior in the N_2 isotherms and their *t* curves, indicat-

(18) Sing, K. S. W.; Everett, D. H.; Haul, R. A. W.; Moscou, L.; Pierotti, R. A.; Rouquerol, J.; Siemieniewska, T. *Pure Appl. Chem.* **1985**, *57*, 603.

(19) (a) Hanzawa, Y.; Suzuki, T.; Kaneko, K. *Langmuir* **1994**, *10*, 2857. (b) Kaneko, K.; Ishii, C. *Colloids Surf.* **1992**, *67*, 203.

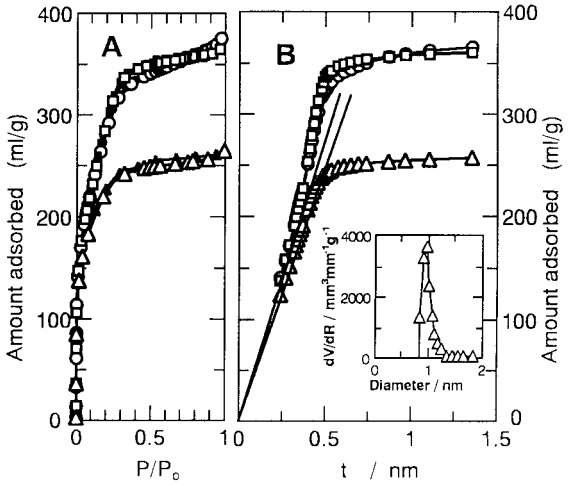

Figure 5. (A) Nitrogen adsorption and desorption isotherms of calcined Zr−SiHIP(x) at 600 °C with x = (○) 0.94, (□) 1.89, and (△) 4.57; and (B) the corresponding t curves and MP plots of A.

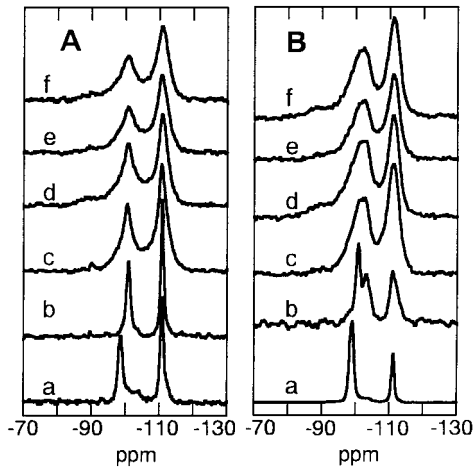

Figure 6. ^{29}Si MAS NMR spectra (A) and CP MAS NMR spectra (B) of (a) H-ilerite, (b) octylamine-intercalated H-ilerite, and as-synthesized products of (c) Si−HIP, (d) Ti−SiHIP(1.98), (e) Al−SiHIP(2.00), and (f) Zr−SiHIP(1.89).

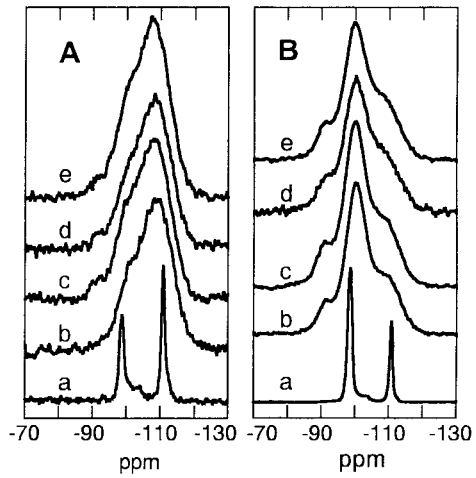

Figure 7. ^{29}Si MAS NMR spectra (A) and CP MAS NMR spectra (B) for (a) H-ilerite, and the calcined products at 600 °C of (b) Si−HIP, (c) Ti−SiHIP(1.98), (d) Al−SiHIP(2.00), and (e) Zr−SiHIP(1.89).

ing that these products should be microporous materials with a broad pore size distribution. On the other hand, Ti−SiHIP(0.98, and 1.98), Al−SiHIP(4.48) and Zr−SiHIP(4.57) with a higher content of Al and Zr give the typical t curves for microporous materials.[16,17] The porous properties such as BET surface area (S_{BET}), and pore volume (V) including the micropore surface area (S_{int}), and micropore diameter (D) for microporous materials are given in Table 1. Since the S_{BET} of H-ilerite was 21 m^2/g, the large S_{BET} of the pillared products (Table 1) would be attributed to the pillar formation between the silicate layer based on many previous reports.[9,20]

As mentioned above, with an increasing amount of introduced metal in the pillar structure, the pillar configuration and therefore porosity is changed, and S_{BET} is significantly decreased. For the microporous products with a higher content of metal, the mean pore diameter was obtained from the MP plots with a sharp pore size distribution as shown in Figures 3B, 4B, and 5B. S_{BET} tends to decrease with increasing calcination temperature due to destruction of part of the pillars, and the calcined products even at 800 °C have a relatively high S_{BET} (486−728 m^2/g).

^{29}Si MAS NMR Spectra. Figure 6A shows the ^{29}Si MAS NMR spectra for the as-synthesized M−SiHIP(x), Si−HIP including H-ilerite and octylamine-intercalated H-ilerite. The corresponding ^{29}Si CP MAS NMR spectra are shown in Figure 6B. The spectrum of H-ilerite exhibits two peaks and one shoulder peak at chemical shifts of −99 ppm (and −104 as a shoulder) and −111 ppm. These can be assigned to the Q^3 [Si(OSi)$_3$(OH)] and Q^4 [Si(OSi)$_4$] structural units, respectively.[21] The Q^3 peaks shift upfield while Q^4 is not affected upon intercalation of octylamine into H-ilerite. The spectra of Si−HIP and M-SiHIP are very similar and appear at the same position as those of the octylamine-intercalated H-ilerite accompanied by broadening, and in addition, weak and broad Q^2 peaks are observed at ca. −90 ppm assigned to the Q^2 [Si(OSi)$_2$(OH)$_2$] structural units.[21] It is obvious that the appearance of Q^2 and the broadening of Q^3 and Q^4 should be attributed to the intercalated TEOS, although we cannot discriminate the detailed contribution to each structural unit between the pillar precursor and the silicate framework of H-ilerite. These observation results are also the case for the corresponding calcined products as shown in Figure 7. On the other hand, the similarity of the spectra between Si−HIP and M−SiHIP as mentioned above indicates that every pillar precursor has nearly the same structure between the layers, and moreover, the corresponding pillars formed upon calcination also have almost the same structure.

Compared to the ^{29}Si MAS NMR spectrum of Si−HIP in Figure 6A, the relative intensity of the (Q^2 + Q^3) to Q^4 sites for the corresponding M−SiHIP(x) increase as much as 1.5 times for Ti−SiHIP(1.98), 1.3 for Al−SiHIP-(1.82), and 1.2 for Zr−SiHIP(2.52). Furthermore, Figure 7A reveals that the Q^2 peaks of M-SiHIP are clearer

(20) (a) Pinnavaia, T. J. *Science* **1983**, *220*, 365. (b) Yamanaka, S.; Nishihara, T.; Hattori, M. *Mater. Chem. Phys.* **1987**, *17*, 87. (c) Vaughan, D. E. W. *Catal. Today* **1988**, *2*, 187. (d) Sequeira, O. A. C., Hudson, M. J., Eds. *Multifunctional Mesoporous Inorganic Solids*; Kluwer Academic Publishers: The Netherlands, 1993; pp 237−258; pp 273−287.

(21) Engelhardt, G.; Michel, D. *High-Resolution Solid-State NMR of Silicates and Zeolites*; John Wiley: New York, 1987.

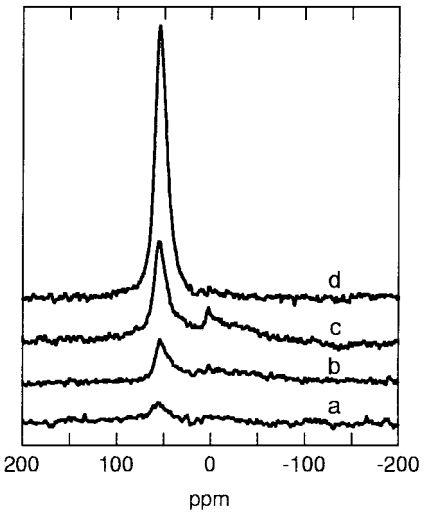

Figure 8. ^{27}Al MAS NMR spectra of (d) as-synthesized Al−SiHIP(4.48), and calcined products at 600 °C of (a) Al−SiHIP-(0.79), (b) Al−SiHIP(2.00), and (c) Al−SiHIP(4.48).

than that of Si−HIP. These behaviors can be explained by the similar influence of the −OH and −OM groups on the chemical shift of the central Si atoms,[22] indicating the contribution of the Si−O−M bridges in the framework of the silica-based pillars.

^{27}Al MAS NMR Spectra. Figure 8 shows the ^{27}Al MAS NMR spectra of the mixed-pillar precursor before calcination (a) and after calcination (b−d). The spectra of every Al−SiHIP composite before calcination consisted of single peaks from the 4-coordinate structural aluminum at ∼55 ppm as shown in Figure 8a.[23] The line at ∼0 ppm ascribed to the nonstructural 6-coordinate aluminum is missing.[23] Upon calcination the NMR spectrum of the higher Al-containing pillared compound gives a line at ∼55 ppm along with an additional weak line at ∼0 ppm as shown in Figure 8c. On the other hand, the other Al−SiHIPs with a lower Al content exhibit a line at ∼55 ppm and the band at ∼0 ppm was almost negligible. The weak additional line at ∼0 ppm for the calcined samples are indicative of 6-coordinate Al. These spectral data indicate that the as-synthesized Al−SiHIP contains only aluminum in the pillar framework as 4-coordinate Al before calcination, although a small amount of Al is removed from the pillar structure upon calcination in the case of the Al-rich product.

UV−Vis Spectroscopy. UV−vis spectroscopy has successfully been used to determine the degree of isolation of Ti and Zr ions incorporated into the silicate framework. Figure 9A shows that UV−vis spectra of Ti−SiHIP under ambient conditions along with those of TS-1 and anatase. It is well-known that the absorption band at ∼210 nm observed for TS-1 is attributed to the ligand-to-metal charge transfer (LMCT) from an O^{2-} to an isolated Ti^{4+} ion in a tetrahedral coordination.[24] The broad band centered at 310 nm for anatase is characteristic of the octahedrally coordinated Ti.[24] Ti−SiHIP(0.98) produces the band centered at 220 nm, and

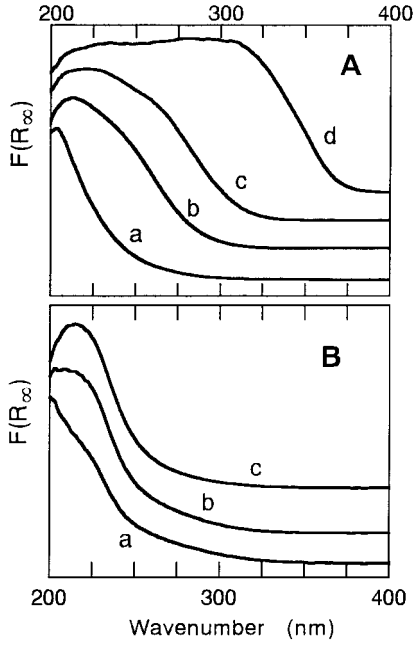

Figure 9. (A) UV−vis spectra of (a) TS-1, and calcined product at 600 °C of (b) Ti−SiHIP(0.98), (c) Ti−SiHIP(1.98), and (d) anatase; and (B) UV−vis spectra of calcined Zr−SiHIP-(x) at 600 °C with x = (a) 0.94, (b) 1.89, and (c) 4.57.

Ti−SiHIP(1.98) exhibits a shoulder at 260 nm along with the 220 nm band. The band at 260−270 nm can be attributed to the presence of Ti atoms in 5- and 6-fold coordinations which are most likely generated through hydration of the tetrahedrally coordinated sites with tetrahedral coordination being most prominent.[25] Hence, the spectrum of Ti−SiHIP shows that Ti isomorphously substitutes for Si in the SiO_4^{4-} tetrahedra of the silica pillar.

Figure 9B shows the UV−vis spectra of Zr−SiHIP with different Zr contents under ambient conditions. With decreasing Zr content, the absorption bands clearly shift toward the shorter wavelengths. The absorption band below 215 nm observed in Zr-containing mesoporous silica and ZSM-5 is assigned to the LMCT transitions in the ZrO_4 tetrahedrally coordinated structures.[26] In ZrO_2 with full connectivity of Zr−O−Zr linkages, the LMCT shifts to the longer wavelength at 230 nm.[26] Similarly, every Zr−SiHIP was found to have an absorption peak below 215 nm accompanied by a small broadening to the lower energy, indicating that most Zr^{4+} ions are isolated into the pillar framework even for the higher content of Zr in this study.

From the ^{29}Si MAS NMR, ^{27}Al MAS NMR, and UV−vis spectra, Al, Ti, and Zr substitute tetrahedrally for Si in the pillar structures formed between the silicate layers. The mixing of the alkoxides in neat octylamine resulted in the formation of a homogeneous solution, which should lead to the high dispersion of metal ions in the silica pillar matrix.

Catalytic Properties. Silica-based mixed oxides of which Si^{4+} is isomorphously substituted by Al^{3+}, Ti^{4+}, or Zr^{4+} ions in the silicate framework are well-known

(22) Liu, Z.; Crrumbaugh, G. M.; Davis, R. J. *J. Catal.* **1996**, *159*, 83.

(23) (a) Luan, Z.; Cheng, C. F.; He, H.; Klinowski, J. *J. Phys. Chem.* **1995**, *99*, 10590. (b) Mokaya, R.; Jones, W. *J. Catal.* **1997**, *172*, 211.

(24) Bordiga, S.; Coluccis, S.; Lamberti, C.; Marchese, L.; Zecchina, A.; Boscherini, F.; Buffa, F.; Genoni, F.; Leofanti, G.; Petrini, G.; Vlaic, G. *J. Phys. Chem.* **1994**, *98*, 4125.

(25) Sinclair, P. E.; Sankar, G.; Richard, C.; Catlow, A.; Thomas, J. M.; Maschmeyer, T. *J. Phys. Chem. B* **1997**, *101*, 4232.

(26) (a) Tuel, A.; Gontier, S.; Teissier, R. *J. Chem. Soc., Chem. Commun.* **1996**, 651. (b) Morrey, M. S.; Stucky, G. D.; Schwartz, S.; Froba, M. *J. Phys. Chem. B* **1999**, *103*, 2037.

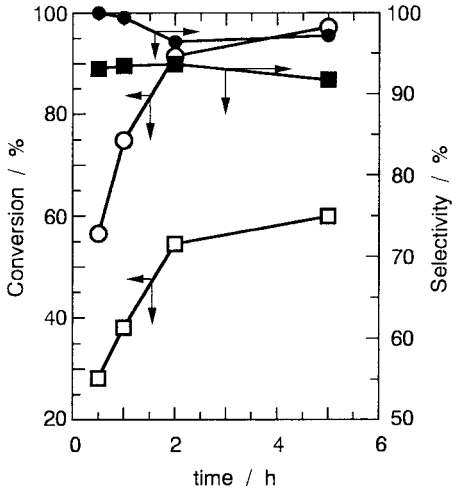

Figure 10. Catalytic activity of Ti−SiHIP(1.98) in the epoxidation of cyclohexene (□) and cyclooctene (○). Conversion (mol %) = (moles of product formed) × 100/(moles of product theoretically expected). Selectivity (mol %) = (moles of epoxide formed) × 100/(total moles of products).

as catalysts in various applications.[14b,15] In this report, only the catalytic reactivity for the epoxidation of cyclohexene and cyclooctene with *tert*-butyl-hydroperoxide (TBHP) on Ti−SiHIP(1.98) was tested and the results are shown in Figure 10. In these reaction conditions, the catalyst shows 96% conversion of cycloctene with 94% epoxide selectivity. The high catalytic potential of Ti−SiHIP is attributed to the isolated Ti atoms in the tetrahedral silica matrix. However, further study is required to obtain a deeper and full understanding for the catalytic properties of Ti−SiHIP including Al−SiHIP and Zr−SiHIP by applying them to various reactions.

Pillar Structure. Pores are classified according to their diameters; micropores below 2 nm, mesopores between 2 and 50 nm, and macropores exceeding 50 nm.[16,18] Understanding of both the porosity from N_2 isotherm studies and the gallery height directly obtained by the basal spacing of XRD patterns and HRTEM images might give pillar configurations. Irrespective of the gallery height of 2−3 nm in every pillared product including Si−HIP, pore size distribution and *t* plot analysis obtained from the isotherms show that these pillared compounds are microporous materials. Furthermore, the microporous products, whose amount of metal is relatively higher, have a uniform micropore size irrespective of the less regularity of the gallery height. These experimental results indicate that the gallery height can be directly determined from the basal reflection in XRD and TEM images, and the corresponding distance between the pillars might be estimated from the pore size distribution calculated from the N_2 isotherms.

From our experimental results, and the conventional investigation on the pillared material,[9,20] our pillar configurations are schematically illustrated in Figure 11. Figure 11a shows a model of Si−HIP which has a uniform gallery height with a low regularity of the two-dimensional pillar array, indicating a low uniformity in the distance between the pillars. This can be expected as Si−HIP has a broad pore size distribution. Due to the introduction of the other metal elements of which

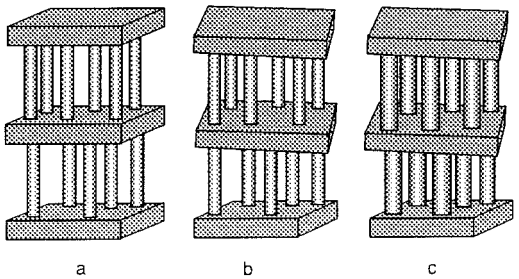

Figure 11. Schematic representation of pillar configuration: (a) a model of Si−HIP which has a uniform gallery height with irregular pillar array; (b) the pillar configuration at lower metal content introduced in the pillar, indicating the irregular gallery height and pillar array; and (c) the state at higher metal content in the pillar, indicating an increase in the thickness of the pillars.

the amount is lower such as Al−SiHIP(0.79 and 2.00) and Zr−SiHIP(0.94 and 1.89), the configuration of the pillars is nearly the same as that of Si−HIP, although the order of the layer-stacking becomes lower as illustrated in Figure 11b. This is evident from the nonuniform lattice fringes of the HRTEM images and relatively broader XRD basal reflection of the Ti−SiHIP sample. The uniform micropore diameter is observed in contrast to the large and irregular gallery height with the increase in metal introduced in the silica-based pillar such as Al−SiHIP(4.48) and Zr−SiHIP(4.57), and the corresponding pillar configuration could be expected as shown in Figure 11c, indicating that the thickness of pillars becomes larger. In the case of Ti−SiHIP, the state of c would be preferentially formed under the lower content of Ti than those of Zr and Al. These differences might be attributed to the cross-linking order of the pillar framework between TEOS and each metal alkoxide used as a starting material.

Conclusion

Ti-, Zr-, and Al-containing silica-pillared compounds of which Si^{4+} is isomorphously substituted by each cation have been prepared from H-ilerite by intercalation of octylamine and the respective mixed alkoxides. The formation of homogeneous alkoxide solutions containing Si and one of the following elements of Al, Ti, and Zr which lead to the high dispersion of metal ions in the silica pillar matrix. The resultant silica-based pillared materials have a BET surface area of about 800m^2/g at 600 °C and have gallery heights of 2−3 nm and the micropore of >2 nm in size between the silicate layers. The increase in the amount of metal introduced into the silica-based pillars was accompanied by a change in the pillar configuration and led to the formation of the microporous products with uniform pore diameters of ∼0.90 nm and the irregular gallery height. With increasing calcination temperature, part of the pillars were destroyed although the calcined products even at 800 °C have a relatively higher S_{BET} of 486−728 m^2/g in contrast to the low S_{BET} of the various pillared smectite clay minerals and pillared layered-metal oxides.

Hence, pillaring of H-ilerite by silica-based mixed oxides has resulted in various metal-containing products with a wide composition range, high specific surface areas, and high degrees of homogeneous metal disper-

sions. This procedure can be used for the synthesis of other metal-containing silica-based pillared materials of which their starting alkoxides are stable as a liquid phase. These new materials should be promising porous materials for use as molecular sieves, adsorbents, catalysts, and other applications. In addition, this procedure would provide a new approach to preparing silica-based porous materials by the pillaring of various layered inorganic materials of which the layer charge is relatively higher.

CM990451M